Site occupancy and valence state of optically active cobalt ions in yttrium iron garnet

B. Antonini,* M. Marinelli, E. Milani,† A. Paoletti,† and P. Paroli†
Istituto di Elettronica dello Stato Solido del Consiglio Nazionale delle Ricerche, Via Cineto Romano 42, I-00156 Roma, Italy

J. Daval and B. Ferrand
Laboratoire d'Electronique et de Technologie de l'Informatique, Centre d'Etudes Nucléaires de Grenoble, Boîte Postale 85X, 30041 Grenoble CEDEX, France
(Received 7 November 1988)

An extensive study is reported of the magneto-optical properties of several film and bulk samples of Co-doped yttrium iron garnet, in the wavelength range 0.65–2.4 μm. The (paramagnetic) nature of all the transitions occurring in this range has been established, and the optical parameters quantitatively determined. The attribution of various transitions to either trivalent or divalent Co has been given, and the (tetrahedral-) site occupancy of the ions involved directly proved by the angular variation of induced anisotropy technique, in several instances. Reducing annealings in hydrogen have been found to reversibly change the valence state of large amounts (up to 90%) of Co^{3+} into Co^{2+}, with consequent strong variations of the associated magneto-optical properties. On the other hand, the annealing and quenching experiments aiming to increase the tetrahedral occupancy of Co ions proved ineffective.

I. INTRODUCTION

Cobalt is one of the most interesting substituents for iron in magnetic garnets. In the divalent state, it is one of the very few ions that can enter *all* garnet cation sites.[1] Also, its overall substitutional range in yttrium-iron garnet (YIG) is as high as 2.5 atoms per formula unit (AFU), namely higher than any other transition-metal ion.[2,3] Over this range, a constant 20% fraction of Co^{2+} enters tetrahedral sites, at least as far as polycrystalline samples made by solid-state reaction at 1400–1450 °C are concerned.

Co^{2+} substitution strongly influences the magnetic properties of YIG, giving rise (for substitutions larger than 1.1 AFU) to compensation points in the thermomagnetic curve,[3] due to different temperature behavior of only the tetrahedral and octahedral sublattices. Much smaller Co^{2+} substitutions have been found to affect the coercive field of Tb-Y iron garnet,[4] as well as the magnetic anisotropy[3–7] and the magnetostriction[7] of YIG. The latter properties are due to the spin-orbit coupling of Co^{2+} ions, much higher than that of the "spherical" Fe^{3+} ions. Indeed, Co^{2+} substitutions as small as 0.01 AFU are sufficient to change[8] the easy magnetic axis of YIG from $\langle 111 \rangle$ to $\langle 100 \rangle$. For such concentrations, a broad first-order reorientational phase transition has been observed,[8] occurring in the temperature range 140–350 K.

Trivalent cobalt can also be substituted in garnets, though to a lower extent than Co^{2+}, and enters tetrahedral and octahedral sites.[9] Octahedral Co^{3+} is a high-spin diamagnetic state.[6] Tetrahedral Co^{3+} gives a negative contribution to the anisotropy constants,[6] and has been shown[10] to yield a strong "growth-induced" magnetic anisotropy in garnet films grown by liquid-phase epitaxy (LPE). Such anisotropy is attributed to partial ordering of Co^{3+} ions along the growth direction, and can be annealed away by thermal treatments, which redistribute Co^{3+} ions randomly.[10]

Cobalt ions give a number of structures in the optical absorption α, both in the visible and in the near infrared;[11] several of the latter fall in the "optical window" of YIG (wavelength λ from 1.1 to 5.0 μm). These structures are attributed[11] to crystal-field "*d-d*" transitions, occurring within Co ions of various valences and site occupancies. Such transitions are, in principle, forbidden by the spin selection rule and also, for ions sitting in octahedral sites, by the parity selection rule. As a consequence, the per-ion optical activity of tetrahedral Co is expected[12] to be about 2 orders of magnitude larger than that of octahedral Co. The former, yet being about 4 times less abundant than the latter, should therefore give a substantially larger contribution to the optical spectra.

The Faraday rotation θ_F associated with Co ions in garnets has been studied by several authors[13–17] with rather contradictory conclusions about the character of the observed transitions, especially for what concerns the spectral region $1.0 \leq \lambda \leq 1.8$ μm. This region is of considerable interest for integrated optics, since magneto-optical garnets could play an important role as basic material for active elements like isolators, switches, and deflectors.[18] All such devices require a high value of θ_F and of the "figure of merit" $R = \theta_F / \alpha$. In Co-substituted garnet films, θ_F values as high as 3×10^3 deg cm^{-1} have been reported,[15] with $R = 4$ deg dB^{-1}. Recently, the optical and magneto-optical properties of Co substituted in other oxides, such as spinels[19,20] and hexaferrites,[20] have also been studied, in connection with applications in the areas of magneto-optical information storage and spectrally selective solar-energy absorbers.

TABLE I. Characteristics of bulk and film samples utilized in the present study. For film samples the total thickness of the two films grown on the two substrate faces is reported.

Sample	Type	Doping	Co concentration (AFU)	Platelet orientation	Thickness (μm)
1	film	Co	0.1	(111)	7.68
2	film	Co+Zr	0.1	(111)	9.42
3	film	Co+Ge	0.17	(100)	15.3
4	bulk	Co	0.01	(110)	490
5	bulk	Co	0.01	(110)	50
6	bulk	Co+Si	0.05	(110)	170

The need to reach a definitive clarification of the structural and magneto-optical properties of Co ions in YIG was our motivation to undertake an extensive study, on both bulk single crystals and epitaxial films, whose results are reported in this paper. All transitions observed for $0.65 \leq \lambda \leq 2.5$ μm are unambiguously shown to be of *paramagnetic* character, in accordance with Ref. 14 and at variance with Refs. 13 and 15. Two of the most magneto-optically active ones, in the range $0.65 \leq \lambda \leq 1.3$ μm, are for the first time *demonstrated* to take place in *tetrahedral* Co^{2+} and Co^{3+}, as first assumed in Ref. 11. Moreover, we have found that, in Co-doped YIG, up to 90% of the tetrahedral Co^{3+} present in the as-grown state can be reversibly changed into Co^{2+} by annealing in hydrogen atmosphere, with relevant effects on the optical and magneto-optical properties. Attempts to change the Co distribution between octahedral and tetrahedral sites were instead unsuccessful, unlike what has been found for Al^{3+} and Ga^{3+} ions.[21,22]

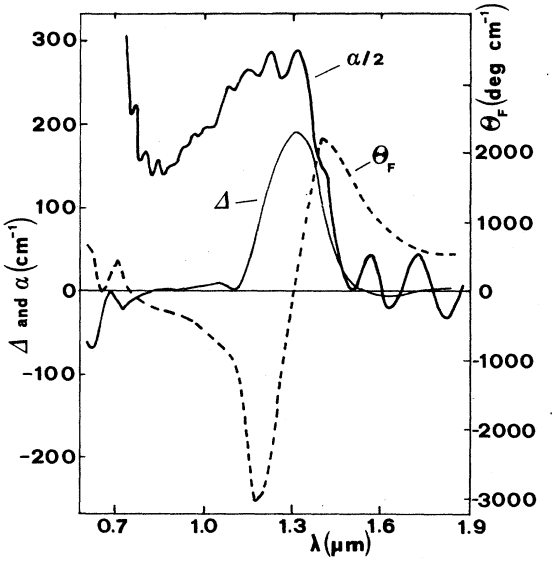

FIG. 1. Spectra of the optical absorption α (thick curve), magnetic circular dichroism Δ (thin curve), and Faraday rotation θ_F (dashed curve) of sample 1 (YIG:Co film; see Table I).

II. EXPERIMENT

Bulk crystals of Co- and (Co+Si)-substituted YIG (indicated in the following as YIG:Co and YIG:Co,Si) were grown, using 99.99%-pure chemicals, from PbO-PbF_2-B_2O_3 fluxed melts,[23] while epitaxial films of YIG:Co, YIG:Co,Zr, and YIG:Co,Ge were grown by LPE techniques from PbO-B_2O_3 melts.[24] Co concentrations of the films were determined by microprobe analysis, and those of bulk samples consequently estimated, by comparison of the magnitude of the optical spectra. Dopings, crystal orientations, and thickness of samples are listed in Table I.

The optical absorption α was measured by a double-beam Cary 17 DI spectrophotometer, while the magnetic circular dichroism Δ was measured by a field-switching technique described elsewhere.[25] The Faraday rotation θ_F up to $\lambda = 1.8$ μm was measured by a polarization-modulation method involving a photoelastic modulator and a Ge photodiode, while for the range $1.7 \leq \lambda \leq 2.5$ μm a new beam-splitting method (described in detail elsewhere[26]) was employed, which allows the use of a PbS photocell. Magnetic linear dichroism measurements (in connection with the angular variation of induced anisot-

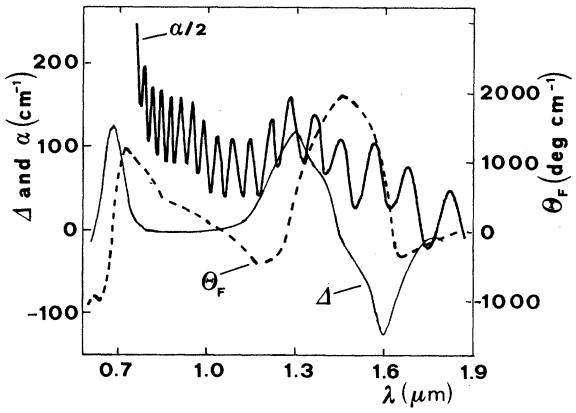

FIG. 2. Spectra of the optical absorption α (thick curve), magnetic circular dichroism Δ (thin curve), and Faraday rotation θ_F (dashed curve) of sample 2 (YIG:Co,Zr film; see Table I).

ropy technique, see Sec. II B) were performed essentially as in Ref. 27. Annealings were performed in 99.99%-pure H_2 or O_2, in horizontal tubular furnaces allowing temperature stability better than 1 °C.

III. RESULTS AND DISCUSSION

A. Optical and magneto-optical spectra

Measured α (corrected for reflectivity), Δ, and θ_F spectra of sample 1 (YIG:Co film), sample 2 (YIG:Co,Zr, film), sample 4 (YIG:Co, bulk), and sample 6 (YIG:Co,Si bulk) are shown in Figs. 1–4. The spectrophotometric α curves of film samples are modulated by interference fringes, due to multiple reflections of the measuring light beam at the film-substrate and film-air interfaces. Comparison of the spectra of samples 1 and 4 with those of samples 2 and 6 clearly indicates that the addition of a tetravalent dopant (namely Si^{4+} or Zr^{4+}) to Co strongly enhances the optical activity around $\lambda=0.7$ and 1.6 μm with respect to YIG:Co, in accordance with early results[11] on Co-doped yttrium gallium and yttrium aluminum garnets (YGG and YAG, respectively). Film samples contain a Co concentration rather larger than bulk ones, so that they are more conducive to the detailed study of the magneto-optical character of the Co transitions, which is a matter of controversy among previous reports.[13–17]

It is well known[28] that the dielectric tensor $\underline{\epsilon}$ of a structurally cubic crystal, magnetized along the z axis, takes the form

$$\underline{\epsilon}=\begin{bmatrix} \epsilon_0 & i\epsilon_1 & 0 \\ -i\epsilon_1 & \epsilon_0 & 0 \\ 0 & 0 & \epsilon_0 \end{bmatrix}, \tag{1}$$

and that the magneto-optical observables Δ and θ_F are related to the real and imaginary parts of ϵ_1 by

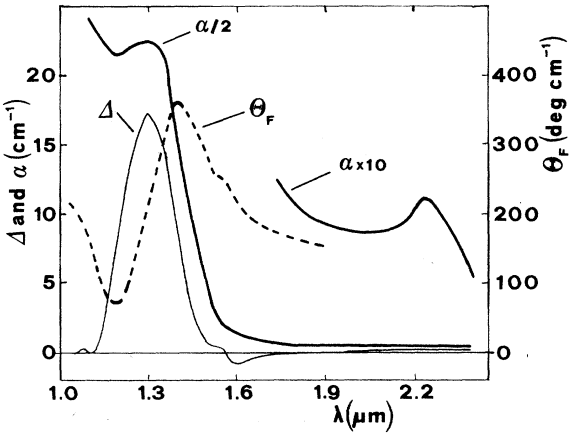

FIG. 3. Spectra of the optical absorption α (thick curve), magnetic circular dichroism Δ (thin curve), and Faraday rotation θ_F (dashed curve) of sample 4 (YIG:Co bulk, see Table I).

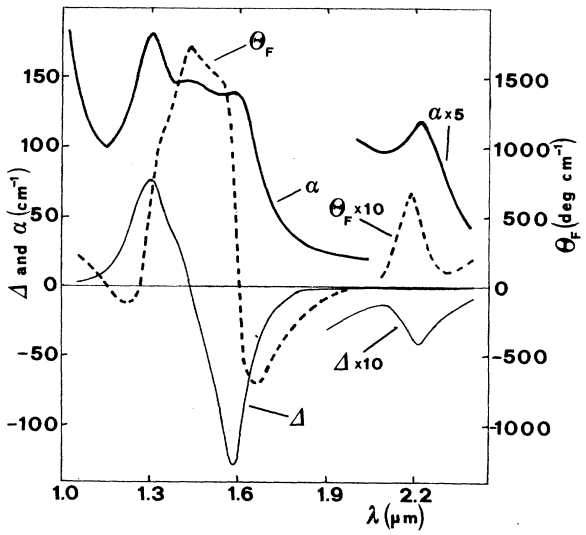

FIG. 4. Spectra of the optical absorption α (thick curve), magnetic circular dichroism Δ (thin curve), and Faraday rotation θ_F (dashed curve) of sample 6 (YIG:Co,Si bulk; see Table I).

$$\epsilon_1'=\frac{\lambda}{\pi}\left[n\theta_F+\frac{k}{4}\Delta\right],$$
$$\epsilon_1''=-\frac{\lambda}{\pi}\left[k\theta_F-\frac{n}{4}\Delta\right], \tag{2}$$

where $n+ik$ is the average complex refraction index for circularly polarized light, and in the hypothesis that $t\Delta \ll 1$ (t being the sample thickness) which is fulfilled in our case. If (as is usually the case) $n \gg k$, Eqs. (2) can be approximated as

$$\theta_F=\frac{\pi}{\lambda}\frac{\epsilon_1'}{n},\quad \Delta=\frac{4\pi}{\lambda}\frac{\epsilon_1''}{n}, \tag{3}$$

namely, the Faraday rotation and the circular dichroism have the same spectral behavior as the imaginary and real parts of the off-diagonal element of the dielectric tensor.

Two main kinds of transitions occur, termed[29] "paramagnetic" and "diamagnetic," which microscopically result from a single excited state and an excited-state doublet, respectively. In the paramagnetic case, Δ is peaked at the transition frequency ω_0, while θ_F has a "dispersive" shape around ω_0, according to the formulas [obtainable from Eqs. (3)]

$$\Delta^{(\text{para})}=C_\Delta\frac{\omega\Gamma(\omega_0^2+\omega^2+\Gamma^2)}{(\omega_0^2-\omega^2+\Gamma^2)^2+4\omega^2\Gamma^2},$$
$$\theta_F^{(\text{para})}=C_F\frac{\omega^2(\omega_0^2-\omega^2-\Gamma^2)}{(\omega_0^2-\omega^2+\Gamma^2)^2+4\omega^2\Gamma^2} \tag{4}$$

(here $\Gamma \ll \omega_0$ is the half width at half maximum of the transition and C_Δ and C_F are amplitude constants).

The corresponding formulas for the diamagnetic case are[29]

$$\Delta^{(\mathrm{dia})}=C'_{\Delta}\frac{\omega\Gamma(\omega_0-\omega)}{[(\omega_0-\omega)^2+\Gamma^2]^2}\ ,$$
$$\theta_F^{(\mathrm{dia})}=C'_F\frac{\omega[(\omega_0-\omega)^2-\Gamma^2]}{[(\omega_0-\omega)^2+\Gamma^2]^2}\ , \tag{5}$$

so that the Δ and θ_F line shapes are roughly interchanged with respect to the paramagnetic case. More precisely, $\Delta^{(\mathrm{dia})}$ has a dispersive shape very similar to $\theta_F^{(\mathrm{para})}$; $\theta_F^{(\mathrm{dia})}$ is peaked at ω_0, as is $\Delta^{(\mathrm{para})}$, but, differently from the latter, undergoes two sign changes at $\omega=\omega_0\pm\Gamma$.

When several transitions occur at close energies, their line shapes may superimpose, making the unambiguous identification of the transition character on the basis of θ_F measurements alone difficult, as in Refs. 13–15. Simultaneous consideration of the θ_F and Δ spectra is a much more reliable procedure. It was previously[29,30] adopted (in a qualitative approach) to study the optical properties of Fe^{3+} ions in YIG and later quantitatively applied[31] to study Fe^{4+} ions in YIG itself.

We have therefore undertaken a quantitative fit of formulas (4) and (5) to the magneto-optical spectra of samples 1 and 2. They were depurified by the contribution of the substrate and of the Fe^{3+} ions of the YIG matrix by subtracting the spectra of a pure YIG film and a GGG substrate (properly weighted).

The starting point was to fit the θ_F and Δ spectra of sample 1, which is expected to contain essentially only Co^{3+} ions. After a qualitative examination (and according to Refs. 13–15) these spectra seem to consist of a single paramagnetic transition at $\lambda\simeq1.3$ μm. However, a good fit to the data could be obtained by only adding two more paramagnetic transitions, occurring at $\lambda=1.1$ and 1.48 μm. Then, we fitted the data of sample 2 (also rich in Co^{2+} ions), allowing further transitions to occur at $\lambda=0.7$ and 1.6 μm. Finally, all transitions having been individualized, all the θ_F and Δ spectra of both samples 1 and 2 have been fitted *simultaneously,* by varying only three parameters for each transition. In fact, for a given transition, the values of ω_0 and Γ must obviously be the same in each of the four spectra; moreover, C_F and C_Δ or C'_F and C'_Δ are not independent: It can be seen that, when θ_F is measured in deg cm^{-1} and Δ in cm^{-1}, it is

$$r'=C'_F/C'_\Delta=7.16\quad r=C_F/C_\Delta=2r'=14.32\ .$$

Of course, two amplitude parameters, K_1 and K_2, have been added, which give the concentration ratios of Co^{3+} and Co^{2+} ions between the two samples.

The curves resulting from the fit are shown in Figs. 5 and 6, and the best-fit parameters are listed in Table II. Since the high-energy part of the spectrum is affected by tails due to transitions (either of Co or Fe ions) occurring above 2 eV, two more transitions have been allowed there, which were located by the fit at 2.29 and 2.54 eV. Of course, no definite meaning can be attributed to these.

Our conclusions are at variance with those of the authors of Refs. 13 and 15, who assign the θ_F peak at about $\lambda=1.5$ μm to a diamagnetic transition occurring at this wavelength, while it clearly results from the superposition of two *dispersive* curves, associated with paramagnetic transitions. Moreover, Ref. 15 also misinterprets the paramagnetic character of the transition at $\lambda=0.7$ μm.

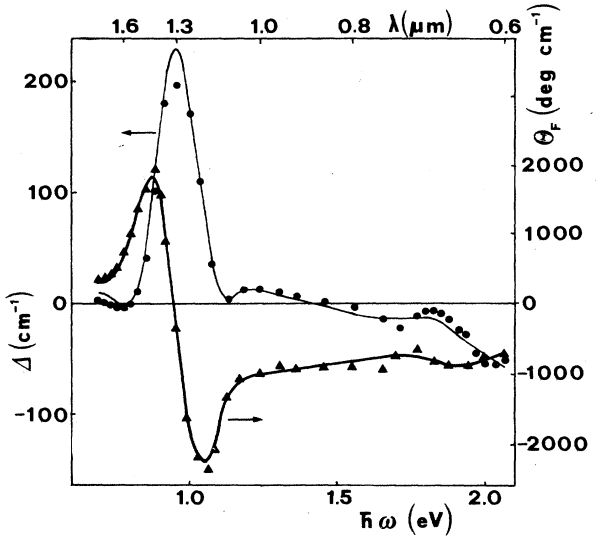

FIG. 5. Result of the best fit to the experimental magneto-optical data of sample 1 (see Sec. III A). Magnetic circular dichroism Δ, dots and thin curve; Faraday rotation θ_F, triangles and thick curve. The best-fit parameters are listed in Table II.

The three main transitions at $\hbar\omega_0=0.78$, 0.94, and 1.83 eV agree with the findings of Ref. 14. However, a subsequent paper[17] by the same author reports a rather different set of transitions, apparently derived from an improper fitting procedure: it seems indeed that the amplitude parameters have been left free to vary *independently,* even for transitions attributed to the same ion. This leads to scarcely understandable results, such as several sign changes of the amplitude parameters (C_F in our notation) relative to the same transition in different samples.

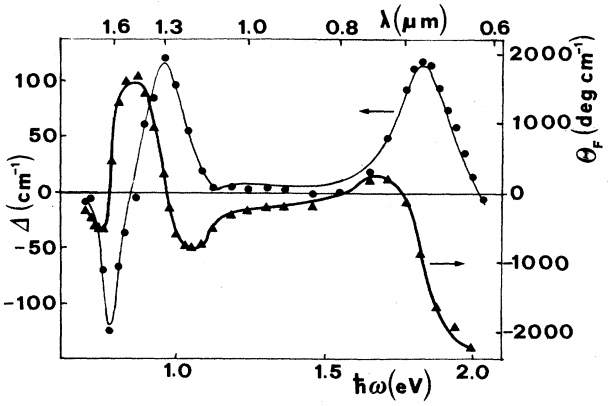

FIG. 6. Result of the best fit to the experimental magneto-optical data of sample 2 (see Sec. III A). Magnetic circular dichroism Δ, dots and thin curve; Faraday rotation θ_F, triangles and thick curve. The best-fit parameters are listed in Table II.

TABLE II. Best-fit parameters obtained for the optical transitions (1–5) of Co ions in YIG. Transitions 6 and 7 have been introduced to take into account the "tails" of transitions (either of Co or Fe ions) occurring at higher energies, outside the measured region (see text).

Transition	Transition energy $\hbar\omega_0$ (eV)	Transition wavelength λ (μm)	Magneto-optical character	Ion	C_Δ	Transition width Γ^2 (eV^2)
1	0.775	1.60	para	Co^{2+}	−1.24	9.2×10^{-4}
2	0.840	1.48	para	Co^{3+}	−13.78	6.20×10^{-3}
3	0.941	1.32	para	Co^{3+}	54.02	9.02×10^{-3}
4	1.10	1.13	para	Co^{3+}	−6.00	3.41×10^{-3}
5	1.83	0.68	para	Co^{2+}	2.17	1.39×10^{-2}
6	2.29		para	see text	−2.84	2.07×10^{-3}
7	2.54		dia		−33.07	3.27×10^{-1}

$$K_1=[Co^{3+}]_{\text{sample 2}}/[Co^{3+}]_{\text{sample 1}}=0.52$$

$$K_2=[Co^{2+}]_{\text{sample 2}}/[Co^{2+}]_{\text{sample 1}}=7.97$$

Figure 4 shows enlarged plots of α, Δ, and θ_F around $\lambda=2.15$ μm. The fact that Δ and α are peaked at the same wavelength, around which θ_F has a dispersive shape, clearly indicates the paramagnetic character of this transition. The much larger amplitude of this transition in sample 3 (doped with Co and Si) with respect to sample 4 (doped with Co alone) seems to support its attribution to divalent Co, in accordance with the conclusion of Ref. 11. However, its behavior under reducing annealing contradicts this conclusion (see Sec. III C). Finally, the data in Fig. 5 show a small but definite paramagnetic transition at $\hbar\omega_0=1.7$ eV, which is attributed to Co^{3+} ions, being absent in Co^{2+}-rich samples (see Fig. 6).

B. AVIA spectra

The angular variation of induced anisotropy (AVIA) is a magneto-optical technique developed by Tucciarone,[32] which proved very effective in determining the site occupancy of several magneto-optically active ions.[27,33–35] The basic idea of AVIA is that the magnetic linear dichroism originated by an active center should show, in principle, symmetry features related to the local symmetry of the site occupied by the center itself.

Let us refer specifically to the problem of identifying the site occupancy of magneto-optically active Co ions in YIG, namely of distinguishing between tetrahedral and octahedral occupancy,[3] in a system where tetrahedral and octahedral sites are distorted along ⟨100⟩- and ⟨111⟩-type axes, respectively.[9] In the pure "axial mode,"[32] the magneto-optically active centers are assumed to possess complete axial symmetry along the local distortion axis so that the absorption of polarized light can be expressed as

$$\alpha(\mathbf{E},\mathbf{m})=\text{const}\times\sum_r(\mathbf{E}\cdot\mathbf{u}_r)^2(\mathbf{m}\cdot\mathbf{u}_r)^2\ , \tag{6}$$

where $\mathbf{E}$ and $\mathbf{m}$ are the unit vectors defining, respectively, the light-polarization direction and the magnetization direction, and $\mathbf{u}_r$ are the unit vectors parallel to the local distortion axes [$\mathbf{u}_1=(1,0,0)$, $\mathbf{u}_2=(0,1,0)$, and $\mathbf{u}_3=(0,0,1)$ for tetrahedral centers; $\mathbf{u}_1=(1,1,1)/\sqrt{3}$, $\mathbf{u}_2=(1,-1,1)/\sqrt{3}$, $\mathbf{u}_3=(1,1,-1)/\sqrt{3}$, and $\mathbf{u}_4=(-1,1,1)/\sqrt{3}$ for octahedral centers]. To distinguish between tetrahedral and octahedral occupancy, a very useful geometry consists of using a (0,0,1) platelet sample, a light beam impinging on it normally [namely $\mathbf{E}\perp(0,0,1)$], and in rotating the magnetization in plane [namely $\mathbf{m}\perp(0,0,1)$]. Then, for instance, for the linear dichroism $\delta\alpha$ between the direction of the magnetization and the perpendicular one, $\delta\alpha=\alpha(\mathbf{E}\parallel\mathbf{m})-\alpha(\mathbf{E}\perp\mathbf{m})$, Eq. (6) yields

$$\delta\alpha(\theta)=\begin{cases}\text{const}\times\cos^2(2\theta) & \text{for tetrahedral centers}\ , \quad (7a)\\ \text{const}\times\sin^2(2\theta) & \text{for octahedral centers}\ , \quad (7b)\end{cases}$$

where θ is the angle between the magnetization direction $\mathbf{m}$ and the [100] axis. Therefore, the $\delta\alpha(\theta)$ behavior clearly discriminates between the two occupancies and $\delta\alpha_{100}=\delta\alpha(\theta=0)$ and $\delta\alpha_{110}=\delta\alpha(\theta=\pi/4)$ at a certain wavelength are proportional to the tetrahedral and octahedral populations of the centers which absorb at that wavelength.

In a recent study the range of validity of the axial model and of the AVIA technique has been quantitatively investigated.[36] The axial model has been found to hold, provided the energy splitting δ due to the local uniaxial distortion is larger than the spin-orbit splitting γ, or, classically speaking, provided the anisotropy associated with the local environment of the center is larger than the anisotropy induced by the magnetization direction. In the opposite case, the $\delta\alpha(\theta)$ is nonzero for any θ, and rather flat, so no information on the site localization of the optical centers involved can be obtained. It can be concluded that, in determining the site occupancies, the AVIA technique may be occasionally noninformative, but *never misleading* in the sense that, if the $\delta\alpha(\theta)$ curve

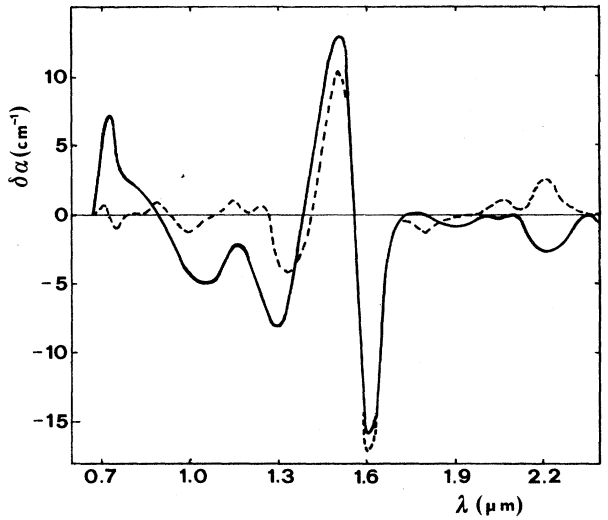

FIG. 7. AVIA spectra (see Sec. III B) of sample 3. Solid curve, "tetrahedral contribution" $\delta\alpha_{100}$; dashed curve, "octahedral contribution" $\delta\alpha_{110}$.

is found to substantially follow a $\sin^2\theta$ or $\cos^2\theta$ behavior, it does indicate the correct site localization, according to Eqs. (7).

Figure 7 shows the $\delta\alpha_{100}$ and $\delta\alpha_{110}$ spectra of sample 3, namely (see Table I) of a (100)-oriented YIG:Co,Ge film. It is evident that $\delta\alpha_{100} > \delta\alpha_{110}$ for the transition at $\lambda = 0.7$ μm and those at $\lambda = 1.1$ and 1.3 μm, while $\delta\alpha_{100} \simeq \delta\alpha_{110}$ for the transitions at $\lambda = 1.48$ and 1.6 μm, as well for the transition at $\lambda = 2.2$ μm. The AVIA response is, therefore, that the transitions at $\lambda = 0.7$ μm and the two at $\lambda = 1.1$ and 1.3 μm [attributed to Co^{2+} and Co^{3+}, respectively (see Sec. III A)] surely occur in tetrahedral sites, while nothing can be said of the others. This is the first direct experimental evidence of the fact that the optical activity around 0.7 and 1.3 μm is due to tetrahedral Co^{2+} and Co^{3+}, as long *assumed* by Wood and Remeika,[11] on the basis of crystal-field calculations.

C. Annealing experiments

Samples 1, 2, 4, and 6 (see Table I) were subjected to a number of thermal annealings in 99.99%-pure hydrogen atmosphere for several hours, at temperatures $T_a \leq 450$ °C (hydrogen annealings at higher T_a were found to induce structural changes in YIG, see Ref. 37). As found in previous magneto-optical studies of various systems,[22,25,38] the magnetic circular dichroism Δ reveals a more suitable probe than the absorption α to monitor ion-population changes, in that (i) with respect to α, Δ presents narrower (positive or negative) peaks, less likely to superimpose reciprocally, and (ii) its measurement is not affected by interference with reflected beams, even in film samples.

The optical properties of sample 6 (bulk YIG:Co,Si) were completely unaffected by any hydrogen-annealing treatment. Figures 8–10 show the maximum Δ changes obtained in samples 1, 2, and 4. The simultaneous changes of θ_F have been already shown in a previous paper.[39] The effects of all above-mentioned annealings are completely reversible, by heating the samples in O_2 above 600 °C for a few hours.

The changes under annealing shown in Figs. 8–10 are, of course, attributed to transformations of Co^{3+} into Co^{2+} ions, presumably occurring by simultaneous formation of OH^- groups, according to the reaction

$$(Y^{3+})_3(Fe^{3+})_{5-x-y-z}(Co^{3+})_x(Co^{2+})_y(M^{4+})_z(O^{2-})_{12}+(v/2)H_2 \rightarrow (Y^{3+})_3(Fe^{3+})_{5-x-y-z}(Co^{3+})_{x-v}(Co^{2+})_{y+v}(M^{4+})_z(O^{2-})_{12-v}[(OH)^-]_v \ , \quad (8)$$

where M^{4+} denotes a tetravalent ion. Considering the amplitude decrease of the transition at $\lambda = 1.3$ μm (attributed to tetrahedral Co^{3+}; see Sec. III B), such valence change appears to concern about 92% of the as-grown tetrahedral Co^{3+} population in bulk YIG:Co and, in YIG:Co films, larger amounts (about 80%) than in films counterdoped with a tetravalent ion (about 50%). Such a difference can be attributed to the fact that, in the latter samples, the Co^{3+}-Co^{2+} chemical equilibrium is, since the beginning, strongly displaced towards Co^{2+} ions, so that further generation of Co^{2+} ions by hydrogen annealing is more difficult.

In Fig. 8 it is seen that, while the dichroism at $\lambda = 1.3$ μm associated with Co^{3+} decreases by about 150 cm^{-1}, the consequent increase of the dichroism at $\lambda = 0.7$ and 1.6 μm (associated with Co^{2+} ions) amounts only to about 40 cm^{-1}. One can conclude, therefore, that the per-ion magneto-optical activity is higher for Co^{3+} than for Co^{2+} ions (both sitting in tetrahedral sites).

A careful inspection of the magnified part of Fig. 10 shows a peculiar phenomenon. In sample 4, after the H_2 annealing, which changes Co^{3+} ions into Co^{2+}, not only the transition at $\lambda = 1.6$ μm (attributed to tetrahedral Co^{2+}) is enhanced, but a new broader secondary transition at $\lambda \simeq 1.8$ μm appears. In other words, part of the Co^{2+} ions generated from the Co^{3+} by hydrogen annealing appear to be somewhat "anomalous" with respect to the ones present in the as-grown state (see, e.g., Fig. 4), induced by tetravalent ion doping. This effect can be explained as follows: The "anomalous" Co^{2+} ions probably sit in tetrahedral cation sites coordinated by three O^{2-} ions and by an OH^- group generated by the hydrogen annealing, and driven close to the Co^{2+} by electrostatic interaction. Due to the fewer surrounding negative charges, in such a site the crystal field is lower than in a normal tetrahedral site, and the splitting induced in the energy levels of the Co^{2+} is also lower, which shifts the optical transition to longer wavelengths. The ratio of the energy splittings is expected to be close to the total charge ratios, which is verified in this case (1.14 versus

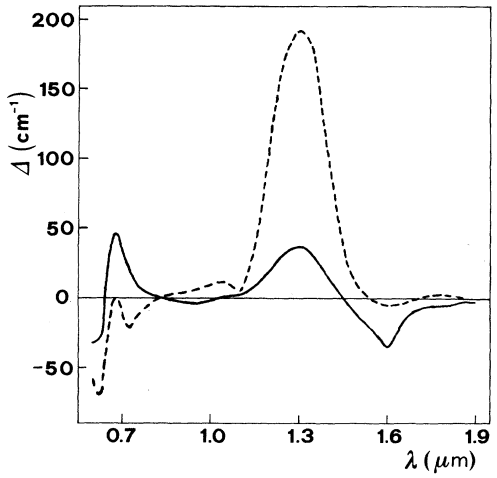

FIG. 8. Change in the spectrum of the magnetic circular dichroism Δ of sample 1 after annealing in hydrogen. Dashed curve, as-grown; solid curve, annealed in hydrogen at 450 °C for saturating times.

1.13). Also, the crystal field of such an "anomalous" site possesses much lower symmetry, actually yielding *several* split optical transitions, which is in agreement with the rather broad secondary peak observed.

If the above explanation is correct, a similar broad secondary peak should be associated with *any* other tetrahedral Co^{2+}-ion transition of sample 4 in the hydrogenated state. Of these transitions, the most prominent is that at $\lambda=0.68$ μm, which, however, is not observable in sample 4 (which is 490 μm thick), due to the high background absorption of the Fe^{3+} ions. We therefore prepared sample 5, a much thinner platelet (50 μm thick), from the same batch as sample 4, and repeated the hydrogen-annealing experiment, monitoring the dichroism in the wavelength range of about 0.7 μm. Figure 11 shows the result: Though the overall spectrum is complicated by the contribution of the Fe^{3+} transitions, a

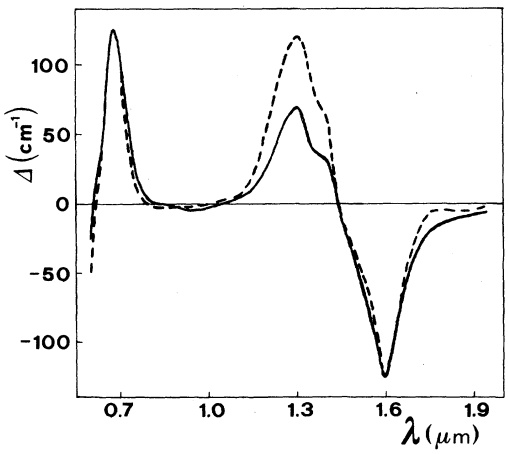

FIG. 9. Change in the spectrum of the magnetic circular dichroism Δ of sample 2 after annealing in hydrogen. Dashed curve, as-grown; solid curve, annealed in hydrogen at 450 °C for saturating times.

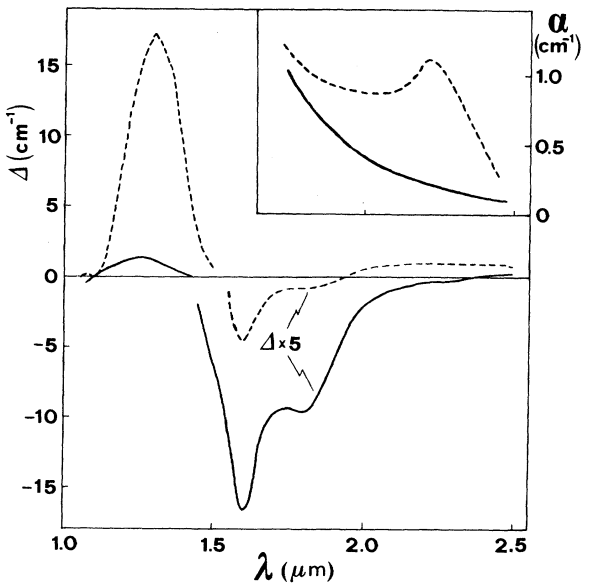

FIG. 10. Change in the spectrum of the magnetic circular dichroism Δ of sample 4 after annealing in hydrogen. Dashed curve, as-grown; solid curve, annealed in hydrogen at 450 °C for saturating times. Inset: corresponding change of the optical absorption α due to the transition occurring at 2.2 μm.

secondary broader peak does appear at $\lambda=0.73$ μm, in agreement with the proposed model.

The contribution of such "anomalous" secondary transitions can be seen, at close inspection, also in the annealed spectra of film samples (Figs. 8 and 9), but have there a much smaller amplitude. The reason might be that the films, grown at temperatures about 200 °C lower than the bulk, incorporate significant amounts of Pb^{2+} from the growth melt,[40] and that OH^- groups might prefer to locate close to Pb^{2+} ions rather than to Co^{2+} ions.

The Δ change under annealing (see inset, Fig. 10) shows that the transition at $\lambda=2.2$ μm disappears as a consequence of the reduction treatment. On the basis of

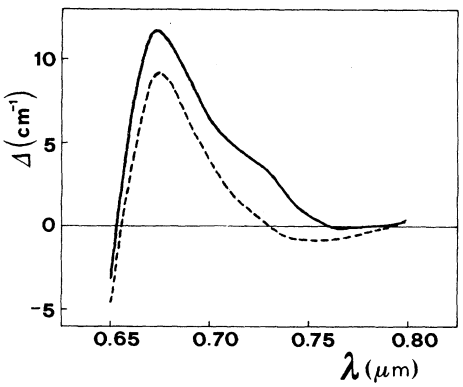

FIG. 11. Change of the magnetic circular dichroism Δ (around the transition at 0.68 μm) of sample 5 after annealing in hydrogen. Dashed curve, as-grown; solid curve, annealed in hydrogen at 450 °C for saturating times.

Eq. (8), it should instead increase, if due to Co^{2+}, as previously concluded[11] on the basis of crystal-field calculations, and from the behavior under counterdoping with Si^{4+} (see Sec. III A). This leaves the question of the attribution of this transition quite open.

Finally, a series of annealing and quenching experiments was performed, with the aim of promoting Co-Fe ion exchange between tetrahedral and octahedral sites. These phenomena are well known to occur for Ga-Fe and Al-Fe ions.[21,22] Since Co ions have a greater preference than Fe^{3+} ions for octahedral versus tetrahedral sites,[3] on the basis of Ref. 21 one would expect the pairs, octahedral Fe plus tetrahedral Co, to correspond to a higher-energy state than the pairs octahedral Co plus tetrahedral Fe. The former should, therefore, increase with respect to the latter if the sample is equilibrated at sufficiently high temperatures and then quenched to room temperature. An increase of the magneto-optical activity in the visible and in the near infrared should result, as this is the major part of the activity associated with tetrahedral Co (see Sec. III B).

To avoid inducing valence changes of Co, these annealings were all performed in oxygen atmosphere, at temperatures up to 1150 °C for film samples (at which temperature the films started being damaged) and up to 1300 °C for bulk samples, for times up to 48 h. The quenching was done by suddenly withdrawing the samples, which were held on a small piece of thin platinum foil, from the furnace, to minimize the thermal capacity. The time required to cool the sample below 900 °C, where no fast-ion exchange is expected,[21] is estimated to be a few seconds. As a monitor of the effects of the annealings, the magnetic circular dichroism Δ was adopted, measured before and after each treatment in the same zone of the sample. All these experiments gave negative results, in that no definite Δ change was ever observed. Our experimental sensitivity is to rule out such variations in the concentration of tetrahedral Co larger than 0.4% of the as-grown population, at least under the experimental conditions described above.

IV. CONCLUSIONS

An extensive study has been performed of the magneto-optical properties of Co ions in YIG, in the spectral range 0.6–2.4 μm, which is of importance to magneto-optical applications such as active devices for integrated optics. The nature of the main transitions has been established, and the optical parameters quantitatively determined. The attribution to either Co^{2+} or Co^{3+} has been given, and the (tetrahedral) site occupancy of the involved Co ions directly proved in several cases.

The possibility of reversibly changing the valence state of large amounts of Co from the trivalent to the divalent state has been demonstrated. The consequent changes in the magneto-optical spectra can be exploited to tailor the material in view of particular applications.

ACKNOWLEDGMENTS

This work was partially supported by Progetto Finalizzato Materiali e Dispositivi per l'Elettronica a Stato Solido (MADESS) of C.N.R. We thank Mr. G. Luce for skillful technical assistance.

*Also at Dipartimento della Scienza dei Materiali, Università degli Studi di Lecce, I-73100 Lecce, Italy.

†Also at Dipartimento di Ingegneria Meccanica, Seconda Università degli Studi di Roma, Tor Vergata, via Orazio Raimondo, I-00173 Roma, Italy.

[1]S. Geller, C. E. Miller, and R. G. Treuting, Acta Crystallogr. **13**, 179 (1959).

[2]S. Geller, H. J. Williams, G. P. Espinosa, and R. C. Sherwood, J. Appl. Phys. **33**, 1195 (1962).

[3]S. Geller, H. J. Williams, G. P. Espinosa, and R. C. Sherwood, Phys. Rev. **136**, A1650 (1964).

[4]E. A. Nesbitt, S. Geller, G. P. Espinosa, and H. J. Williams, J. Appl. Phys. **35**, 2934 (1964).

[5]T. Okada, H. Sekizawa, and S. Iida, J. Phys. Soc. Jpn. **18**, 981 (1963).

[6]M. D. Sturge, E. M. Gyorgy, R. C. LeGraw, and J. P. Remeika, Phys. Rev. **180**, 413 (1969).

[7]P. Hansen, W. Tolksdorf, and R. Krishnan, Phys. Rev. B **16**, 3973 (1977).

[8]S. Geller, G. Balestrino, A. K. Ray, and A. Tucciarone, Phys. Rev. B **27**, 326 (1983).

[9]S. Geller, Z. Kristallogr. **125**, 1 (1967).

[10]E. M. Gyorgy, L. C. Luther, R. C. LeGraw, and S. L. Blank, J. Appl. Phys. **52**, 2326 (1981).

[11]D. L. Wood and J. P. Remeika, J. Chem. Phys. **46**, 3595 (1967).

[12]C. J. Ballhausen and A. D. Liehr, J. Mol. Spectrosc. **2**, 343 (1958).

[13]K. Egashira and T. Manabe, IEEE Trans. Magn. **MAG-8**, 646 (1972).

[14]Z. Simsa, Czech, J. Phys. B **34**, 78 (1984).

[15]A. Itoh, K. Unozawa, T. Shinohara, M. Nakada, F. Inoue, and K. Kawanishi, IEEE Trans. Magn. **MAG-21**, 1672 (1985).

[16]Y. Toriumi, A. Itoh, K. Unozawa, E. Mizobuchi, K. Katayama, F. Inoue, and K. Kawanishi, J. Magn. Soc. Jpn. Suppl. **11**, 249 (1987).

[17]Z. Simsa, IEEE Trans. Magn. **MAG-23**, 3327 (1987).

[18]For a review, see, e.g., P. Paroli, Thin Solid Films **114**, 187 (1984).

[19]J. W. D. Martens, W. L. Peeters, and H. M. van Noort, J. Phys. Chem. Solids **46**, 411 (1985).

[20]M. Abe and M. Gomi, J. Appl. Phys. **53**, 8172 (1982).

[21]P. Röschmann, J. Phys. Chem. Solids **42**, 337 (1981).

[22]R. V. Pisarev, B. Antonini, P. Paroli, and A. Tucciarone, J. Magn. Magn. Mater. **54-57**, 1391 (1986).

[23]L. G. Van Uitert, W. H. Grodkiewicz, and E. F. Dearborn, J. Am. Ceram. Soc. **48**, 105 (1965).

[24]S. L. Blank and J. W. Nielsen, J. Cryst. Growth **17**, 302 (1972).

[25]B. Antonini, A. Paoletti, P. Paroli, A. Tucciarone, J. F. Dillon, Jr., E. M. Gyorgy, and J. P. Remeika, Phys. Rev. B **12**, 3840 (1975).

[26]M. Marinelli, E. Milani, and P. Paroli, Appl. Opt. **27**, 4360 (1988).

[27]B. Antonini, S. Geller, A. Paoletti, P. Paroli, and A. Tucciarone, Phys. Rev. Lett. **41**, 1556 (1978).

[28]L. D. Landau and E. M. Lifshitz, *Statistical Physics* (Per-

gamon, London, 1968), p. 124.
[29]S. Wittekoek, T. J. A. Popma, J. M. Robertson, and P. F. Bongers, Phys. Rev. B **12**, 2777 (1975).
[30]G. B. Scott, D. E. Lacklison, H. I. Ralph, and J. L. Page, Phys. Rev. B **12**, 2562 (1975).
[31]E. Milani and P. Paroli, J. Magn. Magn. Mater. **72**, 208 (1988).
[32]A. Tucciarone, IEEE Trans. Magn. **MAG-14**, 871 (1978); A. Tucciarone, in *Physics of Magnetic Garnets,* edited by A. Paoletti (North-Holland, Amsterdam, 1978), p. 320.
[33]B. Antonini, S. L. Blank, S. Lagomarsino, A. Paoletti, P. Paroli, and A. Tucciarone, IEEE Trans. Magn. **MAG-17**, 3220 (1981).
[34]B. Antonini, R. Krishnan, A. Paoletti, P. Paroli, R. V. Pisarev, and A. Tucciarone, IEEE Trans. Magn. **MAG-17**, 3223 (1981).
[35]B. B. Krichevtsov, O. Ochilov, and R. V. Pisarev, Fiz. Tverd. Tela (Leningrad) **25**, 2404 (1983) [Sov. Phys.—Solid State **25**, 1380 (1983)].
[36]B. B. Krichevtsov and R. V. Pisarev, Zh. Eksp. Teor. Fiz. **84**, 865 (1983) [Sov. Phys.—JETP **57**, 501 (1983)].
[37]B. Antonini, C. D. Brandle, S. Lagomarsino, A. Paoletti, P. Paroli, and A. Tucciarone, J. Appl. Phys. **55**, 2179 (1984).
[38]B. Antonini and P. Paroli, Phys. Rev. B **28**, 3422 (1983).
[39]J. Daval, B. Ferrand, E. Milani, P. Paroli, IEEE Trans. Magn. **MAG-23**, 3488 (1987).
[40]G. B. Scott and J. L. Page, J. Appl. Phys. **48**, 1342 (1977).